

# Fidelity of the coral Sr/Ca paleothermometer following heat stress in the northern Galápagos

Anson H. Cheung<sup>1</sup>, Julia E. Cole<sup>2</sup>, Diane M. Thompson<sup>3</sup>, Lael Vetter<sup>3</sup>,  
Gloria Jimenez<sup>4</sup>, Alexander W. Tudhope<sup>5</sup>

<sup>1</sup>Department of Earth, Environmental, and Planetary Sciences, Brown University, Providence, RI 02912  
<sup>2</sup>Department of Earth and Environmental Sciences, 1100 N. University Ave., University of Michigan, Ann

Arbor, MI 48109

<sup>3</sup>Department of Geosciences, 1040 E. 4th St., University of Arizona, Tucson, AZ 85721

<sup>4</sup>Chubb Limited, Philadelphia, PA, 19106

<sup>5</sup>School of Geosciences, University of Edinburgh, Edinburgh, UK

## Key Points:

- We present Sr/Ca and Mg/Ca measurements of two corals from the northern Galápagos, spanning 25-30 years following the 1982-3 El Niño event.
- In the faster-growing colony, the Sr/Ca-SST relationship weakens after heat stress.
- Excluding data after the heat stress event from proxy calibration improves temperature reconstruction statistics.

---

Corresponding author: Julia E. Cole, colejul@umich.edu

This is the author manuscript accepted for publication and has undergone full peer review but has not been through the copyediting, typesetting, pagination and proofreading process, which may lead to differences between this version and the [Version of Record](#). Please cite this article as doi: [10.1029/2021PA004323](https://doi.org/10.1029/2021PA004323).

This article is protected by copyright. All rights reserved.

## Abstract

Coral Sr/Ca records have been widely used to reconstruct and understand past sea surface temperature (SST) variability in the tropical Pacific. However, in the eastern equatorial Pacific, coral growth conditions are marginal, and strong El Niño events have led to high mortality, limiting opportunities for coral Sr/Ca-based SST reconstructions. In this study, we present two  $\sim 25$  year Sr/Ca and Mg/Ca records measured on modern *Porites lobata* from Wolf and Darwin Islands in the northern Galápagos. In these records, we confirm the well-established relationship between Sr/Ca and SST and investigate the impact of heat stress on this relationship. We demonstrate a weakened relationship between Sr/Ca and SST after a major (Degree Heating Months  $9^{\circ}\text{C}$ -months) heat stress event during the 1997-1998 El Niño, with a larger response in the Wolf core. However, removing data that covers the 1997-1998 El Niño from calibration does not improve reconstruction statistics. Nevertheless, we find that excluding data *after* the 1997-1998 El Niño event from the calibration reduces the SST reconstruction error slightly. These results confirm that coral Sr/Ca is a reliable SST proxy in this region, although it can respond adversely to unusual heat stress. We suggest that noise in Sr/Ca-SST calibrations may be reduced by removing data immediately following large heat extremes.

## Plain Language Summary

The ratio of strontium to calcium (Sr/Ca) in reef-building coral skeletons has long been recognized to covary with the seawater temperature in which the corals grew and has been measured in many corals to understand past temperature changes. However, there are few examples from the eastern equatorial Pacific, an important region that drives variations in the climate system. Furthermore, this ratio might not reflect temperature as reliably after a heat stress event because of the physiological impacts on calcification processes. To test if Sr/Ca in corals from this region can reflect past temperature reliably and if this coral "thermometer" is compromised by heat stress, we analyze two coral records from the northern Galápagos. We find that Sr/Ca in these corals reflect temperature, but their relationship is weaker following heat stress and during the 21st century portion of our coral records. Although the heat stress event itself does not affect how well we can infer past temperature, using data after the event to establish the Sr/Ca-temperature relationship impacts the accuracy of temperature reconstruction. Our results demonstrate that excluding post-heat stress periods from the intervals during which these chemistry-climate relationships are developed may reduce the uncertainty of the resulting temperature reconstructions.

## 1 Introduction

Paleoclimate records based on the geochemistry of reef-building coral skeletons are critical for understanding tropical Pacific climate variability. The increasing number of coral geochemical records and synthesis studies in recent decades have improved our understanding of unforced and forced sea surface temperature (SST) variability in the tropical Pacific (e.g., Carilli et al., 2014; DeLong et al., 2007; Jimenez et al., 2018; Linsley et al., 2015; Nurhati et al., 2009; Tierney et al., 2015; Wu et al., 2014).

Despite these advancements, the spatiotemporal coverage of coral records remains extremely sparse, particularly in the eastern equatorial Pacific where marginal conditions and strong variability limit coral growth (Cole & Tudhope, 2017). Recent analyses have suggested the relationship between coral geochemistry and SST can be disrupted under extreme environmental conditions such as marine heatwaves (Clarke et al., 2017, 2019; D'Olivo & McCulloch, 2017; D'Olivo et al., 2019; Hetzinger et al., 2016; Leupold et al., 2019; Sagar et al., 2016), which raises the question of the fidelity of these proxy records in capturing extreme conditions. Such limitations in data coverage and proxy uncertainties can hinder our ability to understand SST variability in the tropical Pacific (Comboul et al., 2015; Loope

67 et al., 2020). To assess these challenges and the potential for long SST reconstructions  
68 from marginal reef environments in the eastern equatorial Pacific, we evaluate the impact  
69 of environmental stress on coral Sr/Ca calibration in the northern Galápagos.

70 Coral Sr/Ca is commonly used to reconstruct SST, based on a robust negative rela-  
71 tionship between coral Sr/Ca and SST (hereafter "Sr/Ca-SST relationship") across many  
72 locations (e.g., Corrège, 2006, and references therein). This temperature dependence is also  
73 supported by aragonite precipitation experiments (Gaetani & Cohen, 2006; DeCarlo et al.,  
74 2015). However, the sensitivity of Sr/Ca to SST, as indicated by the linear regression slope,  
75 often differs among coral colonies (Alpert et al., 2016; DeLong et al., 2007; Grove et al., 2013;  
76 Sayani et al., 2019; Wu et al., 2014). This makes coral-based SST reconstruction difficult  
77 when empirical calibration is not possible (e.g., when using fossil corals for reconstruction).  
78 These disparities might partially arise from differences in laboratory and/or data processing  
79 methods, for instance sampling a suboptimal growth track or failing to properly account for  
80 observational uncertainties in the calibration (Alibert & McCulloch, 1997; DeLong et al.,  
81 2013; Reed et al., 2021; Wu et al., 2014).

82 Physiological processes may also impact the fidelity of the Sr/Ca-SST proxy (e.g., Alli-  
83 son & Finch, 2004; Goodkin et al., 2005; Thompson, n.d.). Corals calcify from a fluid within  
84 a semi-enclosed environment (calcifying fluid) (Cohen & McConnaughey, 2003; Cohen &  
85 Gaetani, 2010), and preferentially incorporate or exclude trace elements (TEs) depending  
86 on their partition coefficients ( $K_D$ ) (as reviewed by Thompson, n.d.). For example, Sr in-  
87 corporation is weakly favored in the skeleton ( $K_D$  Sr/Ca  $\sim$  1.1) whereas Mg is strongly  
88 excluded ( $K_D$  Mg/Ca  $\sim$  0.001). As calcification proceeds, therefore, the TE/Ca ratio in the  
89 calcifying fluid represents a balance between calcification and replenishment by ambient sea-  
90 water through both active and passive transport processes (McCulloch et al., 2017; Sevilgen  
91 et al., 2019; Thompson, n.d.). Changes in calcification rate can thus alter the geochem-  
92 ical composition of the calcifying fluid and the TE/Ca of the coral skeleton via Rayleigh  
93 fractionation (Cohen & Gaetani, 2010; Thompson, n.d.). In addition, coral calcifying fluid  
94 geochemistry (and thus calcification) is also governed by active transcellular (i.e., through  
95 cells) and/or paracellular (i.e., between cells) pathways (Allemand et al., 2011; Thompson,  
96 n.d.). In particular, active  $\text{Ca}^{2+}$  pumping (via the Ca-ATPase pump) incorporates  $\text{Ca}^{2+}$   
97 (and  $\text{Sr}^{2+}$  as a by-product, Marchitto et al., 2018) and elevates pH of the calcifying fluid to  
98 maintain aragonite supersaturation of the calcifying fluid (Cohen & McConnaughey, 2003;  
99 Thompson, n.d.).

100 Both Rayleigh fractionation and  $\text{Ca}^{2+}$  active transport affect the ratios of TEs to Ca  
101 in the calcifying fluid, and therefore the TE/Ca ratios in coral skeletons (Cohen & Gaetani,  
102 2010; Gaetani & Cohen, 2006; DeCarlo et al., 2015). The strong statistical relationship be-  
103 tween Sr/Ca and SST across numerous sites highlights that in most cases, these processes do  
104 not significantly impact Sr/Ca-based SST reconstructions. However, stressful environmen-  
105 tal conditions may perturb the normal functioning of the coral's calcification physiology, for  
106 instance by disrupting metabolic and calcification processes, and create skeletal geochemical  
107 anomalies. Here we leverage unusually warm SST in Galápagos during an extreme El Niño  
108 event to document the impact of warming on the coral Sr/Ca-SST relationship.

109 The effects of temperature changes on coral calcification have been widely investigated.  
110 Past studies have documented that increases in average and extreme SSTs can cause the  
111 expulsion of zooxanthellae and coral bleaching (e.g. Hoegh-Guldberg, 1999). This has been  
112 observed in field surveys (Glynn, 1988; Glynn et al., 2015, 2018) and naturally extreme  
113 environments (Camp et al., 2018; Hoadley et al., 2019), and is further supported by growth  
114 rate measurements and stress bands in cores from massive corals (e.g., Barkley et al., 2018;  
115 DeCarlo & Cohen, 2017; Lough & Cantin, 2014). However, corals might be more resilient  
116 to temperature changes than previously thought. Geochemical and skeletal density analyses  
117 of cores from massive corals have suggested acclimatization to heat stress (Carilli et al.,  
118 2012; Clarke et al., 2019; DeCarlo et al., 2019; D'Olivo et al., 2019; Leupold et al., 2019;  
119 Thompson & van Woesik, 2009). Nevertheless, the relevant mechanisms remain disputed,

120 and may include changes in genetics, the metabolic conditions, or the community of coral-  
121 associated microbes, including symbionts (e.g., Gibbin et al., 2018; Jones & Berkelmans,  
122 2010; Palumbi et al., 2014; Ziegler et al., 2017). These studies provide multiple lines of  
123 evidence that changes in temperature can impact coral calcification.

124 Changes in coral calcification rate can impact the Sr/Ca of the calcifying fluid and  
125 the skeleton independent of SST. These non-climatic effects have obvious implications for  
126 using skeletal Sr/Ca to reconstruct SST. For example, mounting evidence suggests that  
127 stressful conditions may disrupt the Sr/Ca-SST relationship (Clarke et al., 2017, 2019;  
128 D’Olivo & McCulloch, 2017; D’Olivo et al., 2019; Hetzinger et al., 2016; Leupold et al.,  
129 2019; Sagar et al., 2016). Previous studies have targeted corals that experienced a known  
130 heat stress event and demonstrated that such stress weakens the Sr/Ca-SST relationship.  
131 This breakdown is temporary: the relationship is usually restored within a year, although in  
132 some cases the disruption of the Sr/Ca-SST relationship can last several years (D’Olivo et al.,  
133 2019). Multiple mechanisms have been put forth to explain the disruption of the Sr/Ca-SST  
134 relationship, including: 1) reduced coral extension, which smooths out the seasonal cycle  
135 immediately after the stress event (Barnes et al., 1995; Gagan et al., 2012; Clarke et al.,  
136 2019), 2) a reduction in active transport via transcellular (e.g., Ca-ATPase) or paracellular  
137 pathways due to energy limitations, which reduces aragonite saturation of the calcifying  
138 fluid (Marshall & McCulloch, 2002), and 3) a reduction in calcification rate, which leads to  
139 a Rayleigh fractionation response (Clarke et al., 2017; D’Olivo & McCulloch, 2017; D’Olivo  
140 et al., 2019).

141 Despite evidence that heat stress can disrupt the Sr/Ca-SST relationship, we lack a  
142 clear mechanistic understanding of how this breakdown occurs and its impact on the fi-  
143 delity of the resulting SST reconstruction. First, most prior studies have focused on corals  
144 from regions with similar mean SST and small SST variations. However, a single coral genus’  
145 heat stress response can vary in magnitude from site to site. Notably, corals accustomed to  
146 greater natural SST variability have been shown to be less susceptible to heat stress (Carilli  
147 et al., 2012; Sully et al., 2019; Thompson & van Woesik, 2009), and may therefore exhibit  
148 more consistent SST-TE/Ca relationships. Second, though evidence suggests the impacts  
149 of heat stress on the Sr/Ca-SST relationship can continue for several years (D’Olivo et al.,  
150 2019), most prior studies have only examined changes in the Sr/Ca-SST relationship during  
151 and immediately after a heat stress event. Thus, the statistics of the Sr/Ca-based SST  
152 reconstruction could be biased for some unknown period following temperature extremes.  
153 Third, the impacts of a disrupted Sr/Ca-SST relationship on Sr/Ca calibration and SST  
154 reconstruction have not been fully explored. Given that recent decades have been char-  
155 acterized by an increase in the frequency and intensity of heat stress (Oliver et al., 2018;  
156 Fröhlicher et al., 2018; Hobday et al., 2016), this disruption may have biased the Sr/Ca-  
157 SST calibrations used to reconstruct the history of SST and related phenomena (e.g., the  
158 El Niño-Southern Oscillation; ENSO). Altogether, these unknowns warrant further study  
159 to understand how the Sr/Ca-SST relationship may change in response to heat stress.

160 In this study, we present TE/Ca records measured in two modern *Porites lobata* corals  
161 collected from Wolf and Darwin Islands in the northern Galápagos archipelago, Ecuador,  
162 where large interannual SST variance, low pH, and high nutrients create marginal conditions  
163 for reef growth (Cortés, 1997; Cortés et al., 2017; Manzello et al., 2008). With these  
164 measurements, we address three overarching questions. First, at these marginal sites, does  
165 coral Sr/Ca exhibit a relationship with SST that is consistent with previous studies? Second,  
166 do heat stress events affect the relationship between Sr/Ca and SST at these sites? And  
167 third, if so, does excluding anomalous intervals improve SST reconstruction?

## 2 Materials and Methods

### 2.1 Eastern Equatorial Pacific and Galápagos Oceanography

The Galápagos archipelago lies along the equator,  $\sim 1000$  km west of South America, in a region of large spatial and temporal environmental variability. A meridional SST gradient crosses the archipelago, with warmer conditions in the north and cooler in the south and west (Figure 1). Two major ocean currents govern the oceanography in the Galápagos: 1) the westward South Equatorial Current that splits into two lobes; and 2) the Equatorial Undercurrent that travels eastward in the subsurface and shoals when it strikes the Galápagos platform (Kessler, 2006).

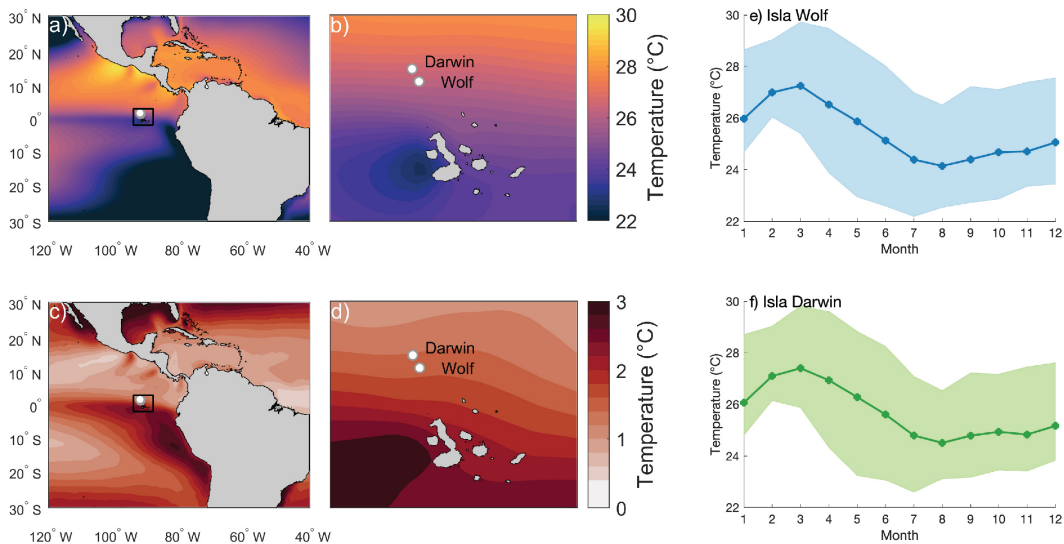


**Figure 1.** Site locations and climatology. a-b) Mean annual SST and c-d) monthly SST standard deviation between 1982-2017 derived from OISST (Reynolds et al., 2007), where b) and d) represent areas enclosed by the boxes in a) and c). e-f) SST climatology of Isla Wolf (GW10-10; blue) and Isla Darwin (GD15-3-1; green) with background color showing SST variations that cover the same span as the Sr/Ca records.

Interannual ENSO extremes can significantly impact Galápagos corals. Both the high temperatures associated with El Niño events and the cooling during La Niñas cause stress and bleaching (Glynn et al., 2015, 2018; Banks et al., 2009). Virtually all coral colonies in the Galápagos archipelago experienced bleaching and mortality following the 1982-83 El Niño (Glynn, 1988); only colonies at Darwin and Wolf Islands showed significant regrowth after the event (Glynn et al., 2015). The 1997-8 El Niño event was also severe, triggering "island-wide" bleaching at Darwin (Glynn et al., 2015); Isla Wolf was not evaluated. Corals in the Galápagos archipelago also frequently experience multi-day rapid cooling events ( $\sim 5-10^{\circ}\text{C}$ ) that are caused by thermocline shoaling (Banks et al., 2009; Riegl et al., 2019a).

### 2.2 Coral Collection and Sampling

We analyzed coral cores from Isla Darwin (core GD15-3-1;  $1^{\circ}42'$  N,  $92^{\circ}$  W) and Isla Wolf (core GW10-10;  $1^{\circ}23'$  N,  $91^{\circ}50'$  W; Figure 1). Both cores were collected from living *P. lobata* coral using diver-operated hydraulic (Wolf) and pneumatic (Darwin) drills, in June 2010 at Wolf and in January 2015 at Darwin. In the lab, we halved, slabbed, and cleaned the cores by sonication in deionized water. Next, we x-rayed the slabs and used the resulting images to establish sampling transects along rapidly growing skeletal "fans" (Figure S1).



193 We also examined two sections of GW10-10 and GD15-3-2 (different core from the same  
194 colony as GD15-3-1) with a scanning electron microscope to screen for diagenesis. Both  
195 sections showed pristine primary aragonite with no evidence of alteration (Figures S2-S3).  
196 We used an automated benchtop mill (Sherline Computer Numerical Control) to subsample  
197 the slabs at 1 mm resolution down core. Earlier measurements from the same powdered  
198 samples (GW10-10) were presented in Jimenez et al. (2018), although that study used a  
199 different ICP-OES instrument and associated methods and only focused on Sr/Ca.

### 200 2.3 Laboratory Methods

201 Our method was modified from Schrag (1999) and Cantarero et al. (2017). For each  
202 sample, 0.5-0.7 mg of coral powder was acidified with 3.5 mL of 5% trace metal grade HNO<sub>3</sub>  
203 to yield a solution of approximately 80 ppm Ca. We measured Sr (421 nm), Mg (285 nm),  
204 and Ca (315 nm) content with a radial torch view using a Thermo Electron Corporation  
205 iCap 7400 Inductively Coupled Plasma - Optimal Emission Spectrometer (ICP-OES) at  
206 the University of Arizona. We computed Sr/Ca and Mg/Ca elemental ratios using Sr (421  
207 nm)/Ca (315 nm), and Mg (285 nm)/Ca (315 nm) output. We corrected the effects of plasma  
208 drift and matrix effects in these elemental ratios following Schrag (1999). To account for  
209 plasma drift, we measured a reference solution between each sample and adjusted the sample  
210 value. Next, in each run, we measured three matrix standards with same TE/Ca but with  
211 different Ca concentrations (60 ppm, 80 ppm, and 100 ppm) created by volumetric dilution  
212 of TE stock solutions; linear regression of measured TE/Ca values on Ca concentration  
213 in matrix standards was used to correct for matrix effects. Afterwards, we normalized  
214 our data by adding the offset between a liquid internal coral standard (MCPL) measured  
215 independently at the University of Western Australia on an ICP-MS and average MCPL  
216 measured value of each run. We also measured two internal coral powder standards (MCP  
217 and JCP-1) to estimate analytical uncertainty.

### 218 2.4 Age Model

219 To construct age models and calibrate our elemental records, we used the 0.25° x  
220 0.25° monthly optimally interpolated sea surface temperature product version 2 (OISSTv2)  
221 (Reynolds et al., 2007). Prior to age modeling, we identified and removed geochemical  
222 outliers following Reed et al. (2021). To establish the age model for GW10-10 and GD15-3-1  
223 elemental records, we identified each year's Sr/Ca minimum and tied it to the corresponding  
224 SST maximum (March) at grid cells 1.625°N, 267.875°E and 1.375°N, 268.125°E for GD15-  
225 3-1 and GW10-10, respectively. Finally, we linearly interpolated each elemental record to  
226 monthly time series based on the annual tie points.

### 227 2.5 Calibration and Residuals

228 We regressed the elemental records onto SST using weighted least squares (WLS) re-  
229 gression based on a maximum likelihood algorithm (Thirumalai et al., 2011; York et al.,  
230 2004) to identify the relationship between TE/Ca records and SST. WLS analysis accounts  
231 for uncertainty in both the SST and elemental time series and allows for correlation in er-  
232 rors. As such, it provides a more robust estimation of the SST-proxy relationship compared  
233 to ordinary least squares regression or reduced major axis regression (Thirumalai et al.,  
234 2011; York et al., 2004). We calculated the analytical uncertainty for each TE/Ca by taking  
235 1 standard deviation ( $1\sigma$ ) of the JCP-1 standard across all runs included in the dataset  
236 ( $n=32$ ).

237 Following linear calibration, we analyzed the residuals from the Sr/Ca-SST regression  
238 to explore whether systematic behavior could be identified. If SST is sufficient to explain  
239 all systematic variations in Sr/Ca, then we expect the residuals to be independent and  
240 follow a normal distribution with zero mean. We determined whether (1) a linear trend  
241 was present in the residual using ordinary least squares regression, (2) the residuals were

242 autocorrelated by analyzing the residuals' autocorrelation function, (3) the residuals were  
 243 normally distributed through an Anderson-Darling test, and (4) the residuals scaled with  
 244 observed SST. The significance of the trend and relationship between residual and observed  
 245 SST were determined by analyzing the standard error of the regression. The significance of  
 246 autocorrelation in the residuals was determined by calculating the large lag standard errors  
 247 at lag  $k$  following Anderson (1976):

$$248 \quad \sqrt{\text{Var}(r_k)} \simeq \sqrt{\frac{1}{N} \left(1 + 2 \sum_{i=1}^K r_i^2\right)} \quad (1)$$

249 where  $N$  = timeseries length,  $r_k$  = correlation at lag  $k$ .

## 250 **2.6 Heat Stress Events**

### 251 **2.6.1 Definition**

252 In Galápagos, heat stress events are commonly associated with strong El Niño condi-  
 253 tions (Figure S4). We defined heat stress events from ERSST version 5 (Huang et al., 2017)  
 254 using the Degrees Heat Month metric (DHM), calculated from a thermal stress threshold  
 255 based on both the maximum climatological temperature and local temperature variability  
 256 (Text S1 and Figure S5; Donner, 2011; Logan et al., 2012). Unlike Degree Heating Weeks  
 257 (Liu et al., 2003), this approach enable us to use monthly SST data. We used ERSST  
 258 because it covers a longer period, permitting a more rigorous assessment of baseline condi-  
 259 tions; nevertheless, its spatial resolution is lower than OISST. As a result of this difference  
 260 in temporal coverage and spatial resolution, the standard deviation of OISST data is larger  
 261 by  $< 0.2^\circ\text{C}$  at both locations, and the mean value is slightly lower (Figure S6). The baseline  
 262 condition ( $SST_c$ ) over the climatological period was defined as:

$$263 \quad SST_c = \langle \max(SST_i) \rangle \quad (2)$$

264 Following Donner (2011), the thermal threshold ( $SST_{2.5\sigma}$ ) was defined as :

$$265 \quad SST_{2.5\sigma} = 2.5 \times \sigma(\max(SST_i)) + SST_c \quad (3)$$

266 where  $\max(SST_i)$  = maximum SST in year  $i$ ,  $\langle \rangle$  = average,  $\sigma$  = standard deviation. We  
 267 defined the climatological period as 1950-1980; hence  $i = 1950, 1951, \dots, 1980$ . The DHM  
 268 of a specific month is defined as the sum of temperature stress (in  $^\circ\text{C}$ ) exceeding this  
 269 threshold ( $SST_{2.5\sigma}$ ) during the current and preceding three months. We used Bleaching  
 270 Alert thresholds defined in Donner (2011) to estimate the likelihood of bleaching due to  
 271 heat stress: Bleaching Alert Level I threshold occurs at  $2.5\sigma(\max(SST_i))^\circ\text{C} \cdot \text{month}$  and  
 272 Bleaching Alert Level II threshold occurs at  $4.9\sigma(\max(SST_i))^\circ\text{C} \cdot \text{month}$ . This approach is  
 273 more robust than the traditional DHM definition because it takes into account the variable  
 274 maximum SST in each year (Donner, 2011; Logan et al., 2012) and evidence that corals are  
 275 less susceptible to extreme conditions when they experience large historical variability (Sully  
 276 et al., 2019; Thompson & van Woesik, 2009). Previous work has also demonstrated improved  
 277 bleaching predictability using this variability-based threshold over traditional DHM (Logan  
 278 et al., 2012).

### 279 **2.6.2 Regression and Jackknifing**

280 We evaluated the impacts of heat stress events on Sr/Ca-SST relationships and SST  
 281 reconstruction using three complementary approaches. First, we calculated running regres-  
 282 sions between Sr/Ca and SST using 5 different moving windows to determine the temporal  
 283 variability of the regression slope (2, 4, 6, 8, and 10 years). Second, we randomly removed  
 284 varying lengths (1, 2, 4, 6, 8, and 10 years) of Sr/Ca and SST data, and used the remaining  
 285 data to perform the regression. This allowed us to identify time periods and interval lengths  
 286 that have the most significant impact on the regression slope. Third, we randomly removed

287 2 consecutive years of Sr/Ca and SST data to mimic the typical length of a heat stress  
 288 event and split the remaining data into halves for calibration and reconstruction. Specif-  
 289 ically, we developed the calibration equation using one half and applied the equation to  
 290 the other half for reconstruction. We then compared the root mean square error (RMSE)  
 291 between the reconstructed SST and instrumental SST. Since the RMSE is sensitive to both  
 292 calibration and reconstruction, we also compared the RMSE using the other half for cali-  
 293 bration/reconstruction. This allowed us to determine if including heat stress events in the  
 294 calibration could influence the reconstruction skill.

### 295 **2.6.3 Rayleigh Fractionation Model**

296 To understand how calcification and active  $Ca^{2+}$  transport changed across the heat  
 297 stress event, we modelled changes in TE/Ca using a closed system Rayleigh fractionation  
 298 equation following Sinclair (2015):

$$299 \left(\frac{TE}{Ca}\right)_{arag} = \left(\frac{TE}{Ca}\right)_{cf} \frac{(1 - P^{K_{D_{TE}}})}{(1 - P)} \quad (4)$$

300 where  $\left(\frac{TE}{Ca}\right)_{arag}$  is the TE/Ca ratio of the skeleton,  $\left(\frac{TE}{Ca}\right)_{cf}$  is the TE/Ca ratio of the  
 301 calcifying fluid, P is the proportion of Ca left in the calcifying fluid after precipitation  
 302 has ended, and  $K_{D_{TE}}$  is the partition coefficient of TE. Following D'Olivo and McCulloch  
 303 (2017), we constructed two equations using Sr/Ca and Mg/Ca data and their respective  
 304  $K_D$  to solve for  $Ca_{cf}$  and P.  $K_D$  for Sr/Ca and Mg/Ca were calculated following  $K_{D_{Sr/Ca}} =$   
 305  $\exp(-1.86 + 600/T_K)$  (Sinclair, 2015) and  $K_{D_{Mg/Ca}} = \exp(-13.13 + 1770/T_K)$  respectively.  
 306 Calculations for  $K_{D_{Mg/Ca}}$  were modified slightly from Sinclair (2015), where  $K_{D_{Mg/Ca}} =$   
 307  $\exp(-12.9 + 1860/T_K)$ , so that P is constrained between 0 and 1 and  $Ca_{cf}$  is higher than  
 308 seawater ( $> 10.25$  mmol/mol).

### 309 **2.7 Age Model Sensitivity Test**

310 We tested the sensitivity of our results to assumptions made in our age model. Our  
 311 age modeling approach assumed that the growth rate was constant between each tie point  
 312 and that maximum SST occurred in March. These assumptions introduce subannual un-  
 313 certainties in our SST reconstruction and can bias the estimated variance (Lawman et al.,  
 314 2020). Thus, we introduced two alternate age models to test the robustness of our results:  
 315 one that tied Sr/Ca minima to observed (not climatological) maximum OISST SST of each  
 316 year, and one that tied Sr/Ca maxima and minima to the observed minimum and maximum  
 317 OISST SST of each year. These two alternate age models explore the impact of subannual  
 318 age model uncertainties stemming from variations in the month when maximum SSTs occur  
 319 each year and the variable seasonal growth rate (explored further in Reed et al. (2021) and  
 320 Wellington and Glynn (1983); Text S2).

## 321 **3 Results and Discussion**

322 The record from GW10-10 spans October 1985 to May 2010, and that from GD15-3-  
 323 1 covers September 1986 to September 2014 (Figure 2). The mean values of Sr/Ca and  
 324 Mg/Ca are comparable between the two cores (GW10-10 Sr/Ca: 9.099 mmol/mol, GD15-  
 325 3-1 Sr/Ca: 9.055 mmol/mol; GW10-10 Mg/Ca: 4.368 mmol/mol, GD15-3-1 Mg/Ca: 4.403  
 326 mmol/mol). The Sr/Ca of GW10-10 exhibits greater variability (standard deviation) than  
 327 that in GD15-3-1 (GW10-10 Sr/Ca: 0.128 mmol/mol, GD15-3-1 Sr/Ca: 0.109 mmol/mol).  
 328 Although the Mg/Ca standard deviation for GW10-10 is also greater than that of GD15-3-1  
 329 GW10-10 Mg/Ca: 0.340 mmol/mol, GD15-3-1 Mg/Ca: 0.256 mmol/mol), this results from  
 330 a single large anomaly that punctuates much lower-variability periods (discussed below).



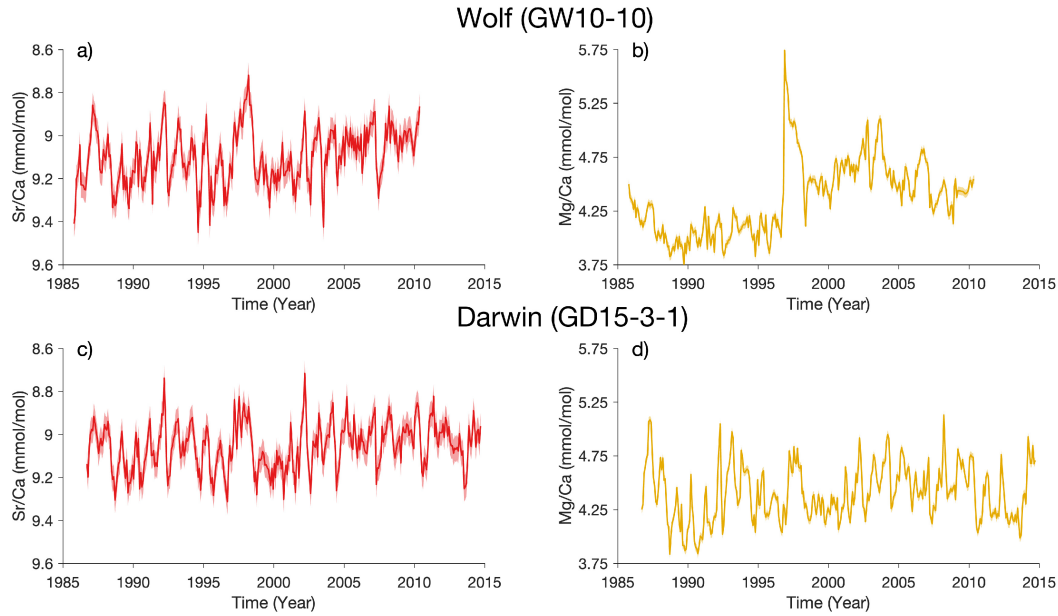


**Figure 2.** Time series of coral records. a) Sr/Ca and b) Mg/Ca time series from GW10-10. c) Sr/Ca and d) Mg/Ca time series from GD15-3-1. Lighter shaded background indicates  $1\sigma$  analytical uncertainty.

### 3.1 Regression and Residuals

WLS regression based on monthly data demonstrates a negative relationship between Sr/Ca and SST at both sites. The regression slopes are  $-0.0625 \pm 0.0024$  and  $-0.0530 \pm 0.0024$  mmol/mol/ $^{\circ}\text{C}$  ( $\pm 1$  standard error) for GW10-10 and GD15-3-1, respectively. A similar relationship between Sr/Ca and SST results from ordinary least squares (OLS) regression (Figure S7).

Sr/Ca calibration of our two records indicate a robust relationship between Sr/Ca and SST. Although the regression slopes are different between the two records, they are within the range suggested in previous synthesis studies (Corrège, 2006) and a previously published Sr/Ca reconstruction from the Galápagos (Jimenez et al., 2018). These results give confidence that Sr/Ca is a reliable paleothermometer at this site (Cole & Tudhope, 2017; Schrag, 1999).

**Table 1.** Statistical moments of GW10-10 and GD15-3-1 Sr/Ca-SST residuals using 1-month and 3-month averaged data

Moments	GW10-10		GD15-3-1	
	1 Month	3 Month	1 Month	3 Month
Mean	-5.9696E-6	-1.7219E-4	8.4963E-5	3.2586E-5
Variance	0.0081	0.0044	0.0066	0.0041
Skewness	0.3511	0.2124	0.1546	0.0246
Kurtosis	3.5637	2.9737	2.8910	2.4863

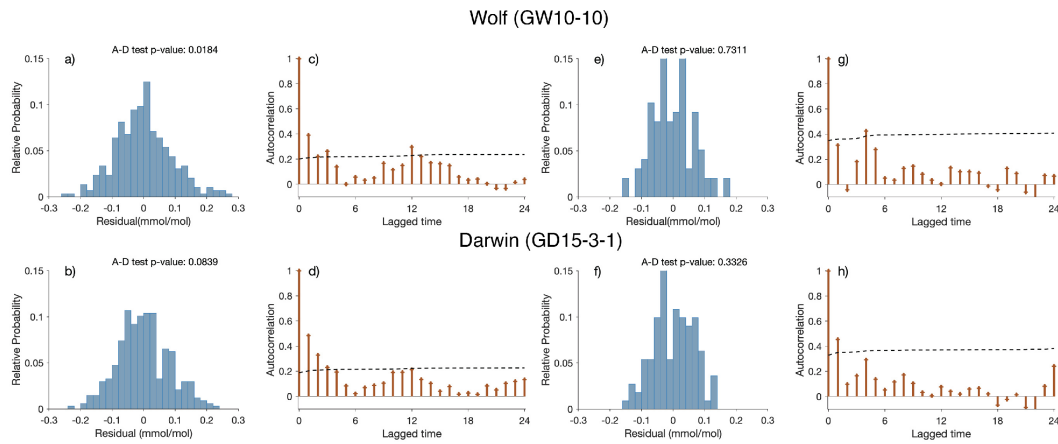


**Figure 3.** Residual characteristics from Sr/Ca calibration. Monthly data: a-b) Residual distribution and c-d) autocorrelation of residuals, with dashed line representing 2 standard error. Three-month averaged data: e-f) Residual distribution, and g-h) autocorrelation of residuals, with dashed line representing 2 standard error. Top row shows results from GW10-10 whereas bottom row shows results from GD15-3-1. Also shown are p-values of the Anderson Darling test.

343 Residuals from the linear regression between Sr/Ca and SST can provide additional insight  
 344 into how well monthly Sr/Ca variations are linearly related to SST and whether factors  
 345 other than SST systematically influence coral Sr/Ca. We analyzed four properties of the  
 346 residuals from the Sr/Ca-SST regression at both sites (Figure 3a-d, S8a-d). The Anderson-  
 347 Darling test indicates residuals from GW10-10 exhibit non-normal behavior, whereas residu-  
 348 als from GD15-3-1 follow a normal distribution. The non-normal GW10-10 residual behavior  
 349 is also reflected in higher order statistical moments (with a positively skewed, leptokurtotic  
 350 distribution, Table 1). The skewness and kurtosis of GD15-3-1 residuals are closer to values  
 351 expected from a normal distribution (Table 1). We also find significant autocorrelation in  
 352 both residuals (up to a 4 month lag). OLS regression of the Sr/Ca residuals as a function  
 353 of time suggests residuals from both sites exhibit a statistically significant negative trend.  
 354 Lastly, the amplitude of the Sr/Ca residual does not scale with observed SST, as indicated  
 355 by the lack of significant correlation between the residuals and SST (Figure S8a-d). The  
 356 non-normal, autocorrelated residuals and the negative temporal trend in residuals violate  
 357 the assumptions made in linear regression and suggest that not all systematic variations in  
 358 Sr/Ca on monthly timescale are linearly related to SST.

359 Such non-normal behavior and autocorrelation in residuals could simply arise from errors  
 360 in the age-depth model (Text S2) or the fact that a linear model cannot fully capture  
 361 Sr/Ca-SST relationship. However, despite a strengthened Sr/Ca-SST relationship using the  
 362 two alternate age models, the negative trend, the autocorrelation (in both cores), and the  
 363 non-normal behavior (in GW10-10) of residuals persist (Figure S9). Furthermore, compar-  
 364 ison between the goodness of fit of a linear, 2<sup>nd</sup> order polynomial, and exponential models  
 365 suggest that applying a higher order model to describe the Sr/Ca-SST relationship does  
 366 not yield statistical benefit (not shown). These results imply that our assumptions related  
 367 to age modeling (constant growth rate between tie points and stationary seasonality) and  
 368 regression model are unlikely to be the only cause of autocorrelation and non-normal residu-  
 369 als, even though small ( $\sim$ monthly) age offsets might systematically bias the Sr/Ca records  
 370 on subseasonal timescales.

371 To reduce the effects of subseasonal age uncertainty from our monthly resolution data,  
 372 we create three-month (‘seasonal’) averages of Sr/Ca and SST centered on March, June,  
 373 September, and December of each year. Next, we regress seasonal Sr/Ca onto seasonal

374 SST for Sr/Ca calibration. This approach reduces autocorrelation in the residuals (Figure  
 375 3e-h) while maintaining subannual resolution. In both cores, the Sr/Ca-SST correlation  
 376 increases and the slope steepens compared to monthly resolution, with regression slopes  
 377 of  $-0.0703 \pm 0.0046$  and  $-0.0580 \pm 0.0046$  mmol/mol/ $^{\circ}\text{C}$  ( $\pm 1$  standard error) for GW10-  
 378 10 and GD15-3-1 respectively (Figure 4). This approach also reduces the skewness and  
 379 kurtosis of residuals in GW10-10 and normalizes the distribution (Table 1). This result is  
 380 consistent with the behavior of residuals in the monthly dataset, where there is significant  
 381 1-4 month lagged correlation (Figure 3). Averaging monthly data to 3-month intervals thus  
 382 minimizes the autocorrelation in the residual, and the 3-month regressions yield a more  
 383 reliable estimate of the Sr/Ca-SST relationship. We present the remaining results based on  
 384 the 3-month (seasonal) averaged data.

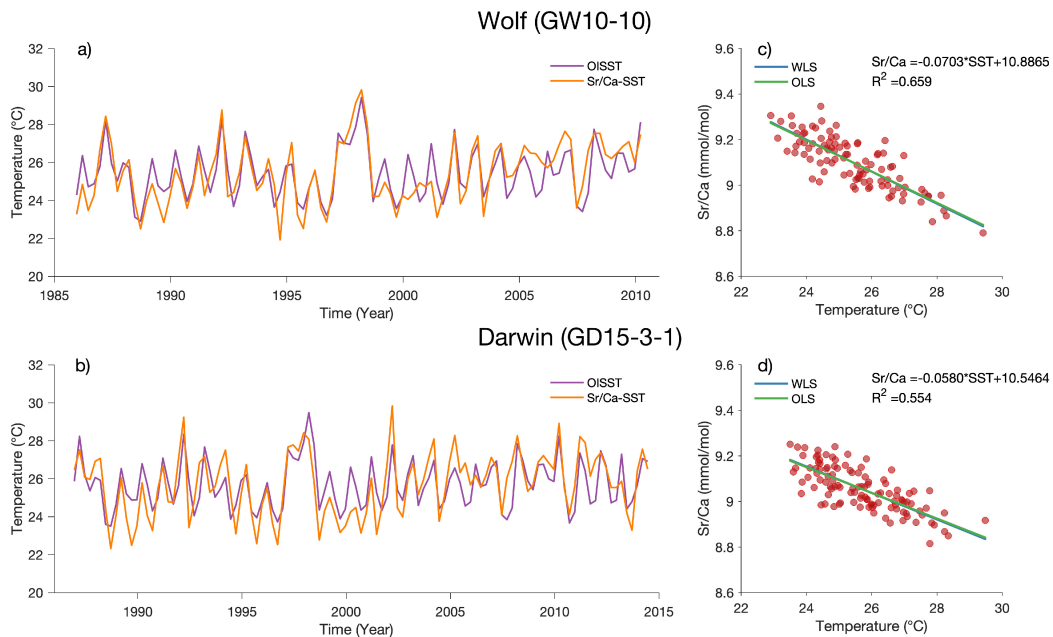


**Figure 4.** 3 month averaged Sr/Ca and SST relationship. Time series of seasonal (Feb-Apr, May-Jul, Aug-Oct, Nov-Jan) instrumental SST and Sr/Ca-inferred SST from a) GW10-10 and b) GD15-3-1. Also shown are Sr/Ca regressed onto SST for c) GW10-10 and d) GD15-3-1 using a weight least square approach (WLS; blue) and ordinary least square approach (OLS; green).

### 3.2 Heat stress and Sr/Ca-SST relationship

385  
 386 Based on the DHM metric, we identify three heat stress events since 1985 (Figure  
 387 5g), which correspond to well-known El Niño events (1987-1988, 1992-1993, and 1997-1998;  
 388 Figure S4). The 1997-1998 event reached Bleaching Alert Level II, whereas 1987-1988  
 389 and 1992-1993 reached Bleaching Alert Level I. Comparing DHM to running regressions of  
 390 Sr/Ca and SST, using varying running window lengths, we observe a weakened Sr/Ca-SST  
 391 relationship after the 1997-1998 El Niño (Figures 5), when massive bleaching was recorded  
 392 (Donner et al., 2017; Glynn, 2000). The reduction is particularly substantial in GW10-10.  
 393 However, both cores capture the magnitude of the 1997-1998 El Niño event in their Sr/Ca  
 394 records with remarkable consistency (Figure 4). Changes in Sr/Ca-SST relationship across  
 395 the other Bleaching Alert I events are not apparent.

396 In contrast to Sr/Ca, Mg/Ca behaves differently in these cores, particularly across  
 397 the 1997-1998 El Niño event. Prior to 1997, Mg/Ca correlates with Sr/Ca and with SST

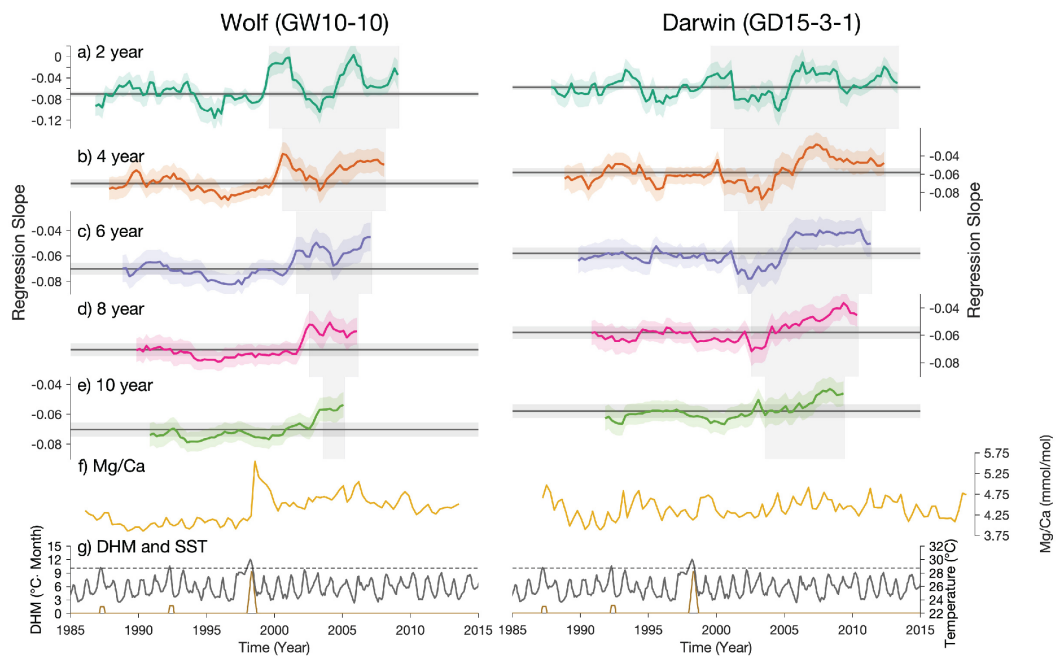


**Figure 5.** 3 month averaged running regression for GW10-10 (left) and GD15-3-1 (right). Regression slopes with a) 2 year, b) 4 year, c) 6 year, d) 8 year, e) 10 year running window. Also shown are f) Mg/Ca, g) DHM (brown) and SST (dark gray) with heat stress threshold (dashed line) for comparison. Black horizontal line and shadings shown in a-e) represent the regression slope obtained using the full dataset and  $1\sigma$  WLS uncertainty, respectively. Shaded area overlaid in each subplot represents periods post-1997 where the 1997-98 El Niño period was not included.

398 in both cores, but its range is much smaller in GW10-10 (Figure 7). In both cores, the  
 399 initial warming in 1997 is accompanied by an anomalous increase in coral Mg/Ca; this is  
 400 particularly notable in core GW10-10 (Figure 6). Following this event, we observe a sharp  
 401 reduction in the Sr/Ca-SST relationship in the 2-year running regression window (Figure  
 402 5), as the Mg/Ca drops to a new baseline level of approximately 0.5 mmol/mol above pre-  
 403 1997 values. In core GD15-3-1, we see a similar change in Mg/Ca ~1997; however, Mg/Ca  
 404 returns to values that are comparable to pre-heat stress after the event, and the change in  
 405 the Sr/Ca-SST relationship is smaller compared to GW10-10.

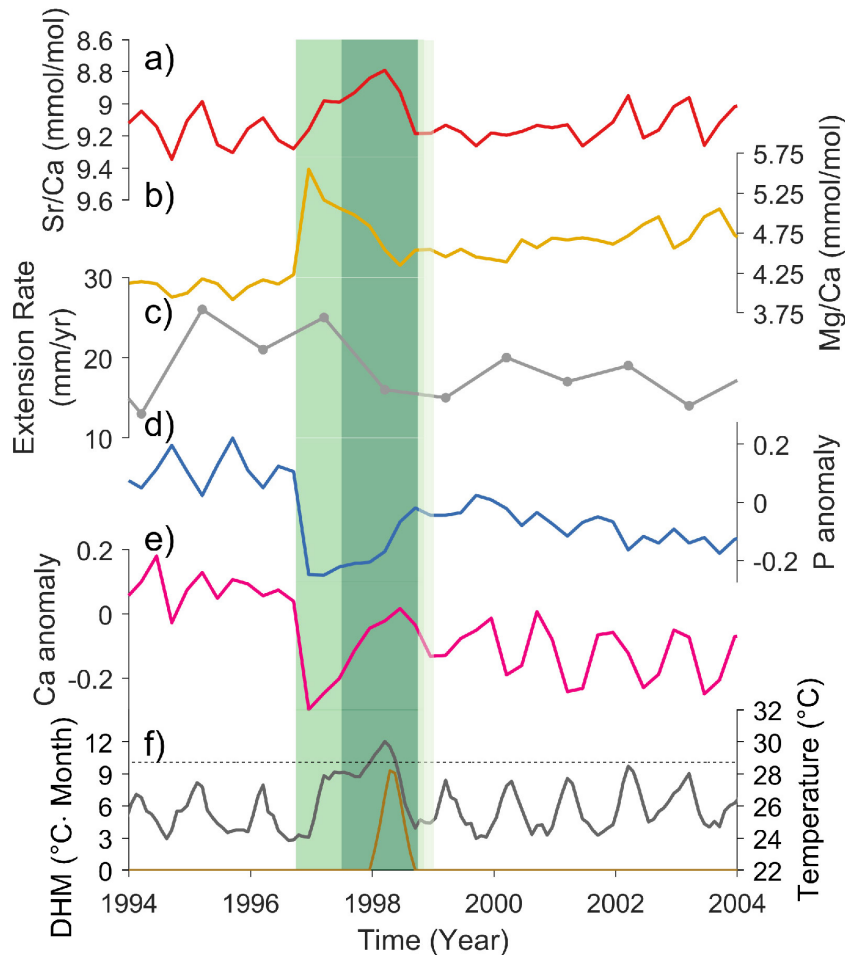


**Figure 6.** GW10-10 changes between 1994 and 2004. Variations of GW10-10 a) Sr/Ca, b) Mg/Ca, c) linear extension rate, d) mean centered proportion of  $Ca^{2+}$  remaining in a batch of calcifying fluid after calcification finalizes (P) e) mean centered concentration of  $Ca^{2+}$  in the calcifying fluid ( $[Ca^{2+}]_{cf}$ ), and f) SST conditions derived from ERSSTv5 between 1994-2004. The green shaded regions indicate the initial rise in Mg/Ca (green), accumulation of heat stress (dark green), and the return to ‘normal’ conditions (light green).

406 Other factors that could impact the Sr/Ca-SST relationship include irregular growth  
 407 patterns that compromise optimal sampling strategy and reduced variance of SST that  
 408 reduces signal/noise. The bottom section of GD15-3-1 was sampled in a region of irregular  
 409 banding (Figure S1). However, we do not observe a shift in regression slope during that  
 410 period (Figure 5). Moreover, the apparent stress response is weaker in the core with the  
 411 more irregular growth (GD15-3-1), supporting the inference that suboptimal sampling does



not play an important role in our results. We also note a reduction in standard deviation in SST and Sr/Ca after 1998, and during the early 1990s (Figure S10-S11). Critically, the weakened Sr/Ca-SST relationship only occurred post-1998. Hence, the weakened Sr/Ca-SST relationship cannot be explained either by suboptimal sampling of irregular growth or by a change in signal to noise ratio over time.

We therefore posit that that coral physiological changes can explain the change in Sr/Ca-SST relationship following the 1997-1998 El Niño that caused regional bleaching. Previous studies have suggested three mechanisms that may weaken the Sr/Ca-SST relationship: a) attenuation of seasonality due to reduced extension rate and biosmoothing (Clarke et al., 2019; D'Olivo et al., 2019), b) reduced active ion transport (e.g., via Ca-ATPase pumping) due to diminished energy or DIC supply (Marshall & McCulloch, 2002), and c) a Rayleigh fractionation response to reduced calcification (Clarke et al., 2017; D'Olivo & McCulloch, 2017). Due to the contrasting pathways by which each are impacted by heat stress, skeletal chemistry and growth changes can be used to distinguish among these mechanisms.

The simplest explanation is that under stress, coral extension slows, and the climate signal is not as finely sampled under a constant-depth, bulk sampling protocol, leading to undersampling the true variance (Barnes et al., 1995; D'Olivo et al., 2019; Gagan et al., 2012; Nothdurft & Webb, 2007). If this explanation were true, the seasonality of Sr/Ca and Mg/Ca would be reduced, but their relationship would not change. However, the relationship between seasonal Sr/Ca and Mg/Ca in GW10-10 changes dramatically after 1998 (Figure 7), indicating that biosmoothing cannot explain the weakening in Sr/Ca-SST correlation across the 1997-1998 heat stress event.

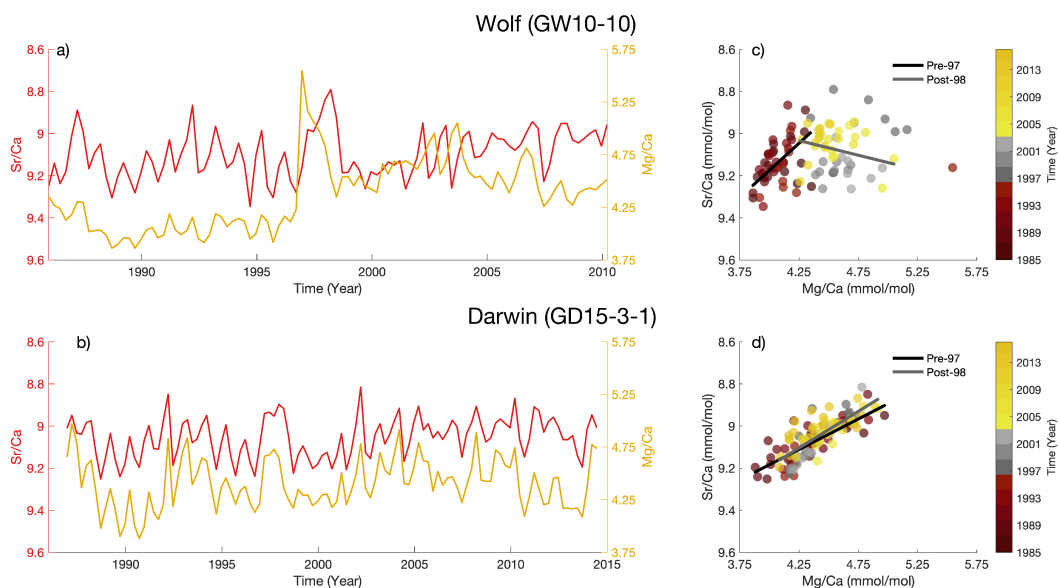


**Figure 7.** Sr/Ca and Mg/Ca relationship. a-b) Time series of 3 month averaged Sr/Ca (red) and Mg/Ca (gold) and c-d) scatter plot of Sr/Ca and Mg/Ca from GW10-10 (top) and GD15-3-1 (bottom). Color in scatter plots represents time as indicated by color bar. Also shown are regression lines calculating using data before 1997 (pre-97) and data after 1998 (post-98). Note that the y-axis of Sr/Ca is reversed.

Alternatively, stress-related changes in active transport by paracellular or transcellular pathways (e.g., Ca-ATPase pumping) may explain the changes we observe. Both pathways require energy for ion transport, and may therefore be impacted by heat stress. However,

437 they have contrasting impacts on TE/Ca ratios: transcellular pathways can concentrate ions  
438 against the electrochemical gradient, whereas paracellular pathways will equilibrate ions  
439 based on the concentration gradient between the calcifying fluid and seawater (as reviewed  
440 by Thompson, n.d.). Evidence for elevated  $[Ca^{2+}]$  in the calcifying fluid (DeCarlo et al.,  
441 2018; Sevilgen et al., 2019) suggests that the Ca-ATPase pump (a transcellular pathway)  
442 is important for ion transport, although the relative contribution of these pathways is still  
443 an active area of research. Using metabolic energy, Ca-ATPase actively pumps  $Ca^{2+}$  into  
444 the calcifying fluid for calcification. Concurrently, two  $H^+$  are removed from the calcifying  
445 fluid, which elevates pH and aragonite saturation by shifting the carbonate reactions to  
446 favor  $[CO_3]^{-2}$  (as reviewed by Thompson, n.d.). Heat stress often causes corals to lose their  
447 symbiotic zooxanthellae (known as bleaching), which lowers the supply of energy available  
448 to power active  $Ca^{2+}$  transport (Marshall & McCulloch, 2002). The loss of metabolic energy  
449 would reduce the supply of  $Ca^{2+}$  to the calcifying fluid and decrease the calcifying fluid pH  
450 and aragonite saturation. This pump is thought to transport Sr similarly to Ca (Marchitto  
451 et al., 2018), but limited data suggest that it discriminates against Mg. Thus a weakened  
452 Ca-ATPase pump would increase the Mg/Ca in the coral skeleton and leave Sr/Ca largely  
453 unchanged. Our Mg/Ca and Sr/Ca data during the heat stress interval are consistent with  
454 a weaker Ca-ATPase pump, especially in the Wolf core (Figure 6). Future work will utilize  
455 a suite of geochemical tracers, including boron isotope systematics, to assess changes in  
456 the pH and aragonite saturation of the coral calcifying fluid following thermal stress and  
457 bleaching.

458 Finally, changes in Rayleigh fractionation can also alter the Sr/Ca-SST relationship in  
459 corals. Rayleigh fractionation occurs due to the difference in partition coefficients among  
460 TEs, and leads to a negative relationship between Sr/Ca ( $K_D \sim 1.1$ ) and Mg/Ca ( $K_D$   
461  $\ll 1$ ) in the coral skeleton (amplified by the temperature dependence of Sr/Ca; Cohen  
462 & Gaetani, 2010; Marchitto et al., 2018; Thompson, n.d.). Increased calcification rates  
463 would drive stronger Rayleigh partitioning, whereas reduced calcification would weaken  
464 it. If calcification slowed as a consequence of reduced Ca-ATPase pumping (i.e., driving  
465 calcification fluid towards lower aragonite saturation and lower pH), we would expect a lower  
466 Mg/Ca and higher Sr/Ca ratio as Rayleigh fractionation weakened (Cohen & Gaetani, 2010).  
467 We observe an anticorrelation between Mg/Ca and Sr/Ca in both cores prior to 1998, and  
468 a weakening/reversal of this relationship in GW10-10 only after 1998 (Figure 7). However,  
469 this weakened relationship is marked by an increase in Mg/Ca, which contradicts what  
470 would be expected from weakened Rayleigh fractionation. This result suggests that reduced  
471 Rayleigh fractionation alone cannot explain the unusual behavior of Sr/Ca and Mg/Ca in  
472 GW10-10.

473 In contrast with our results from Wolf, we see no significant change in the relationship  
474 between Sr/Ca and Mg/Ca before and after the heat stress event in the Darwin record.  
475 Changes in the post-event Sr/Ca-SST relationship are broadly similar to those at Wolf, but  
476 the Mg/Ca anomaly is smaller at Darwin. The reduction in Sr/Ca-SST relationship and  
477 changes in Sr/Ca and Mg/Ca could be a result of weakened Rayleigh fractionation at this  
478 site, but the smaller Mg/Ca anomaly and consistent relationship between Mg/Ca and Sr/Ca  
479 point to a reduced impact of heat on this coral.

480 Taking these results together, we argue that the short-term weakening of the Sr/Ca-SST  
481 relationship in the Wolf record is related to a reduction in available energy as bleaching cut off  
482 photosynthetic energy supplies. This energy loss weakened the Ca-ATPase pump, increasing  
483 Mg/Ca in the calcifying fluid and the skeleton (due to reduced Ca) and minimally impacting  
484 Sr/Ca (because both Sr and Ca are reduced). On the other hand, the slight weakening of the  
485 Sr/Ca-SST relationship and the lack of change in Sr/Ca-Mg/Ca relationship in the Darwin  
486 record suggests that the effects of coral calcification on the Sr/Ca-SST relationship were  
487 small in that colony. Regardless of the dominant mechanism(s), the small impact observed  
488 in GD15-3-1 suggests a stronger resilience to warming.

489 The difference in sensitivity to heat stress between these two corals is interesting. Al-  
490 though environmental variations could theoretically account for this difference, by influenc-  
491 ing the amount of metabolic energy available and altering growth rate, in fact the islands  
492 are very similar in their climate; Wolf is cooler on average ( $\sim 0.5^\circ\text{C}$ ) than Darwin (Riegl et  
493 al., 2019a). Even at Wolf (i.e., within the same growth environment), the extension rates of  
494 different coral colonies vary substantially by ( $\sim 1$  cm/yr; Jimenez et al., 2018; Reed et al.,  
495 2021). These facts imply that environmental differences do not govern the growth rate and  
496 thus the sensitivity to heat stress. We suggest instead that colony-specific factors are more  
497 likely to be responsible for this difference. For example, symbiont taxa have different tol-  
498 erances for temperature change, and the dominant symbiont type can affect corals' growth  
499 rate. If GW10-10 had a more sensitive symbiont type than GD15-3-1, it could have had a  
500 higher growth rate while also experiencing a more substantial loss of the energy powering  
501 the Ca-ATPase pump when under heat stress (Jones & Berkelmans, 2010). The intercolony  
502 difference in geochemistry suggests a greater sensitivity to heat stress in the Wolf colony,  
503 e.g. bleaching or bleaching severity, compared to the one from Darwin.

### 504 3.3 Implications for Sr/Ca-SST calibration

505 Many paleoclimate studies, including this one, rely on the recent SST record for cal-  
506 ibration, when observations are most reliable, but also when heat stress events have been  
507 more frequent and intense (Oliver et al., 2018). Since our results suggest that heat stress  
508 impacts the relationship between Sr/Ca and SST, it is important to determine whether  
509 including heat stress events in the calibration can bias the Sr/Ca-SST relationship used for  
510 SST reconstruction.

511 We quantify the effect of heat stress events on the skill of the reconstruction. Removing  
512 2 years of Sr/Ca-SST data across the 1997-1998 El Niño from the calibration period does not  
513 substantially change the reconstruction skill, as indicated by the RMSE (Figure 8). However,  
514 the reconstruction skill increases when excluding data following the heat stress event to  
515 establish calibration. This result is further corroborated by a more negative regression slope  
516 (i.e., a stronger SST dependence) when data near and after the largest heat stress event  
517 (1997-98 El Niño) are excluded from calculation (Figure S12).

518 Surprisingly, removing only heat stress events from the calibration dataset does not  
519 significantly improve SST reconstruction. Nevertheless, the RMSE is higher when the more  
520 recent part of the dataset is used for calibration, hinting at a long-term shift in the Sr/Ca-  
521 SST relationship in both records (Figure 8). Even though the underlying cause of this shift  
522 cannot be addressed with the data in hand, the fact that these patterns coincide with the  
523 1997-98 El Niño suggest this shift might be a long-term response to heat stress. We note  
524 that the limited length of our datasets ( $\sim 25$  year) undermines our ability to fully quantify  
525 the uncertainty that this post heat stress response would add to a longer SST reconstruction.  
526 Nonetheless, our data suggest the choice of calibration could result in a  $\sim 0.3^\circ\text{C}$  average  
527 difference in reconstruction.

## 528 4 Summary and Conclusion

529 Using seasonal data, we demonstrate that the Sr/Ca-SST relationship in these Galá-  
530 pagos corals is consistent with studies from other regions. We find that a large heat stress  
531 (strong El Niño) event affected the Sr/Ca-SST relationship in one of our two colonies. We  
532 attribute this change to a loss of metabolic energy from photosynthesis during a time of  
533 bleaching, resulting in weakening of the Ca-ATPase pump; we cannot rule out a secondary,  
534 minor attenuation of Rayleigh fractionation. Despite the impacts on the Sr/Ca-SST rela-  
535 tionship, we do not find a significant increase in reconstruction error even when including  
536 this heat stress period. However, we show an improvement in reconstruction skill when  
537 excluding the most recent (post-stress) data from calibration, highlighting the sensitivity of  
538 the reconstruction to the calibration dataset.

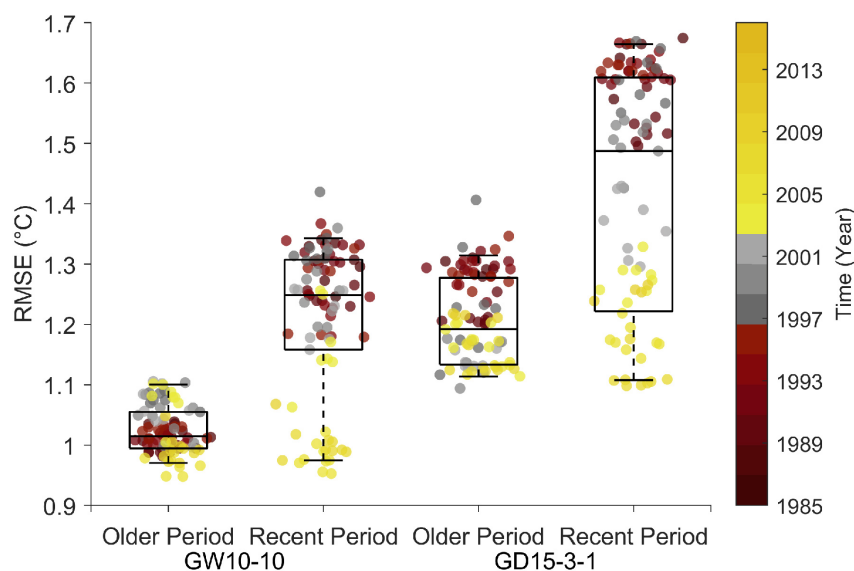


**Figure 8.** RMSE of reconstructed SST. RMSE of reconstructed SST after 2 years of data was removed from GW10-10 and GD15-3-1. The x-axis labels indicate which portion of the data was used for calibration (older: before the removed interval versus recent: after the removed interval). Box and whiskers represent the reconstruction skill (RMSE). The color of the circles indicates the 2 year interval removed before calibration and reconstruction. The RMSE is centered on where the 2 years of data was removed.

539 Our study has three major implications. First, despite the tendency to calibrate Sr/Ca  
 540 with SST at monthly resolution given a sufficient coral growth rate, our analyses suggest  
 541 that this monthly relationship results in larger, non-climate-related residuals. Instead, using  
 542 3-month averaged data for Sr/Ca-SST calibration yields improved (Gaussian) residuals.  
 543 We recommend routine examination of residuals when calibrating proxy to instrumental  
 544 data. Second, the Sr/Ca-SST relationship in these corals is affected by heat stress, even  
 545 in highly variable environments such as the eastern equatorial Pacific; the sensitivity varies  
 546 among individuals. Lastly, although removing the heat stress period does not improve  
 547 SST reconstruction, the SST reconstruction skill increases when data from the post-stress  
 548 period is excluded from calibration, which could reflect a systemic response to heat stress.  
 549 These results imply that calibrating Sr/Ca-SST using the most recent period, when corals  
 550 have experienced greater levels of extreme heat stress, might increase SST reconstruction  
 551 error. We suggest that calibration to instrumental data include analysis of the suitability  
 552 of calibration intervals, not just in terms of instrumental data coverage, but also to exclude  
 553 extreme events that might bias the calibration and resulting climate reconstruction.

#### 554 Acknowledgments

555 We are grateful to the Parque Nacional Galápagos for permission and support to work in this  
 556 very special place, and to the Charles Darwin Research Station for facilitating this project.  
 557 Field sampling was enabled by the crew of the Queen Mabel and her captain Eduardo  
 558 Rosero. Roberto Pepolas particularly improved our local understanding, coring efficiency,  
 559 and safety over multiple field seasons. We also thank Jenifer Suarez, Meriwether Wilson,  
 560 Diego Ruiz, Colin Chilcott, Jorge Baque, and Stephan Hlohowskyj for tireless field assistance  
 561 and expertise. We thank Corey Shaver for her help in laboratory analysis, Emma Reed for  
 562 helpful comments and suggestions, and Juan Pablo D'Olivo for the Rayleigh fractionation  
 563 equation MATLAB code. This work was supported by NSF grants 1401326/1829613 and

564 0957881 to JEC, and by the University of Arizona Honors College Alumni Legacy Grant  
 565 (Honors Thesis) and Brown University Presidential Fellowship to AHC. This publication is  
 566 contribution #2415 of the Charles Darwin Foundation for the Galápagos Islands.

## 567 Open Research

568 All data produced in this study are accessible at the National Center for Environmental  
 569 Information paleoclimatology database at <https://www.ncdc.noaa.gov/paleo/study/33894>.  
 570 The NOAA Physical Sciences Research Lab (Boulder, CO) provided ERSST V5 data  
 571 (<https://psl.noaa.gov/data/gridded/data.noaa.ersst.v5.html>), and NOAA High Res-  
 572 olution SST data were accessed at  
 573 [https://climexp.knmi.nl/select.cgi?id=someone@somewhere&field=sstoiv2\\_monthly](https://climexp.knmi.nl/select.cgi?id=someone@somewhere&field=sstoiv2_monthly)  
 574 [\\_mean](#).

## 575 References

- 576 Alibert, C., & McCulloch, M. T. (1997). Strontium/calcium ratios in modern porites corals  
 577 from the great barrier reef as a proxy for sea surface temperature: Calibration of  
 578 the thermometer and monitoring of enso. *Paleoceanography*, *12*(3), 345-363. doi:  
 579 10.1029/97PA00318
- 580 Allemand, D., Tambutté, É., Zoccola, D., & Tambutté, S. (2011). Coral calcification, cells  
 581 to reefs. *Coral reefs: an ecosystem in transition*, 119–150.
- 582 Allison, N., & Finch, A. A. (2004). High-resolution sr/ca records in modern porites lobata  
 583 corals: Effects of skeletal extension rate and architecture. *Geochemistry, Geophysics,*  
 584 *Geosystems*, *5*(5). doi: 10.1029/2004GC000696
- 585 Alpert, A. E., Cohen, A. L., Oppo, D. W., DeCarlo, T. M., Gove, J. M., & Young, C. W.  
 586 (2016). Comparison of equatorial Pacific sea surface temperature variability and trends  
 587 with Sr/Ca records from multiple corals. *Paleoceanography*, *31*(2), 252-265. doi:  
 588 10.1002/2015PA002897
- 589 Anderson, O. D. (1976). *Time series analysis and forecasting: the box-jenkins approach*  
 590 (Vol. 19). Butterworths London.
- 591 Banks, S., Vera, M., & Chiriboga, A. (2009). Establishing reference points to assess long-  
 592 term change in zooxanthellate coral communities of the northern galápagos coral reefs.  
 593 *Galápagos Research*, *66*, 43–64.
- 594 Barkley, H. C., Cohen, A. L., Mollica, N. R., Brainard, R. E., Rivera, H. E., DeCarlo, T. M.,  
 595 ... others (2018). Repeat bleaching of a central pacific coral reef over the past six  
 596 decades (1960–2016). *Communications biology*, *1*(1), 1–10.
- 597 Barnes, D., Taylor, R., & Lough, J. (1995). On the inclusion of trace materials into massive  
 598 coral skeletons. part ii: distortions in skeletal records of annual climate cycles due  
 599 to growth processes. *Journal of experimental marine biology and ecology*, *194*(2),  
 600 251–275.
- 601 Camp, E. F., Schoepf, V., Mumby, P. J., Hardtke, L. A., Rodolfo-Metalpa, R., Smith, D. J.,  
 602 & Suggett, D. J. (2018). The future of coral reefs subject to rapid climate change:  
 603 lessons from natural extreme environments. *Frontiers in Marine Science*, *5*, 4.
- 604 Cantarero, S. I., T. I. Tanzil, J., & Goodkin, N. F. (2017). Simultaneous analysis of  
 605 Ba and Sr to Ca ratios in scleractinian corals by inductively coupled plasma optical  
 606 emissions spectrometry. *Limnology and Oceanography: Methods*, *15*(1), 116-123. doi:  
 607 10.1002/lom3.10152
- 608 Carilli, J. E., Donner, S. D., & Hartmann, A. C. (2012). Historical temperature variability  
 609 affects coral response to heat stress. *PLoS One*, *7*(3), e34418.
- 610 Carilli, J. E., McGregor, H. V., Gaudry, J. J., Donner, S. D., Gagan, M. K., Stevenson,  
 611 S., ... Fink, D. (2014). Equatorial pacific coral geochemical records show recent  
 612 weakening of the walker circulation. *Paleoceanography*, *29*(11), 1031–1045.
- 613 Clarke, H., D’Olivo, J. P., Conde, M., Evans, R. D., & McCulloch, M. T. (2019). Coral  
 614 records of variable stress impacts and possible acclimatization to recent marine heat



- 615 wave events on the northwest shelf of australia. *Paleoceanography and Paleoclimatol-*  
616 *ogy*, 34(11), 1672-1688. doi: 10.1029/2018PA003509
- 617 Clarke, H., D'Olivo, J. P., Falter, J., Zinke, J., Lowe, R., & McCulloch, M. (2017). Dif-  
618 ferential response of corals to regional mass-warming events as evident from skeletal  
619 Sr/Ca and Mg/Ca ratios. *Geochemistry, Geophysics, Geosystems*, 18(5), 1794-1809.  
620 doi: 10.1002/2016GC006788
- 621 Cohen, A., & Gaetani, G. A. (2010). Ion partitioning and the geochemistry of coral skeletons:  
622 solving the mystery of the vital effect. *EMU Notes Mineral*, 11, 377–397.
- 623 Cohen, A., & McConnaughey, T. (2003). Geochemical perspectives on coral mineralization.  
624 *Reviews in mineralogy and geochemistry*, 54(1), 151–187.
- 625 Cole, J., & Tudhope, A. W. (2017). Reef-based reconstructions of eastern pacific climate  
626 variability. In *Coral reefs of the eastern tropical pacific* (pp. 535–548). Springer.
- 627 Comboul, M., Emile-Geay, J., Hakim, G. J., & Evans, M. N. (2015). Paleoclimate sampling  
628 as a sensor placement problem. *Journal of Climate*, 28(19), 7717 - 7740. doi: 10.1175/  
629 JCLI-D-14-00802.1
- 630 Corrège, T. (2006). Sea surface temperature and salinity reconstruction from coral geochem-  
631 ical tracers. *Palaeogeography, Palaeoclimatology, Palaeoecology*, 232(2-4), 408–428.
- 632 Cortés, J. (1997). Biology and geology of eastern pacific coral reefs. *Coral Reefs*, 16(1),  
633 S39–S46.
- 634 Cortés, J., Enochs, I. C., Sibaja-Cordero, J., Hernández, L., Alvarado, J. J., Breedy, O., ...  
635 Zapata, F. A. (2017). Marine biodiversity of eastern tropical pacific coral reefs. In  
636 P. W. Glynn, D. P. Manzello, & I. C. Enochs (Eds.), *Coral reefs of the eastern tropical*  
637 *pacific: Persistence and loss in a dynamic environment* (pp. 203–250). Dordrecht:  
638 Springer Netherlands. doi: 10.1007/978-94-017-7499-4\_7
- 639 DeCarlo, T. M., & Cohen, A. L. (2017). Dissepiments, density bands and signatures of  
640 thermal stress in porites skeletons. *Coral Reefs*, 36(3), 749–761.
- 641 DeCarlo, T. M., Gaetani, G. A., Holcomb, M., & Cohen, A. L. (2015). Experimental  
642 determination of factors controlling U/Ca of aragonite precipitated from seawater:  
643 Implications for interpreting coral skeleton. *Geochimica et Cosmochimica Acta*, 162,  
644 151 - 165. doi: <https://doi.org/10.1016/j.gca.2015.04.016>
- 645 DeCarlo, T. M., Harrison, H. B., Gajdzik, L., Alaguada, D., Rodolfo-Metalpa, R., D'Olivo,  
646 J., ... McCulloch, M. T. (2019). Acclimatization of massive reef-building corals  
647 to consecutive heatwaves. *Proceedings of the Royal Society B: Biological Sciences*,  
648 286(1898), 20190235. doi: 10.1098/rspb.2019.0235
- 649 DeCarlo, T. M., Holcomb, M., & McCulloch, M. T. (2018). Reviews and syntheses: Re-  
650 visiting the boron systematics of aragonite and their application to coral calcification.  
651 *Biogeosciences*, 15(9), 2819–2834. Retrieved from [https://bg.copernicus.org/  
652 articles/15/2819/2018/](https://bg.copernicus.org/articles/15/2819/2018/) doi: 10.5194/bg-15-2819-2018
- 653 DeLong, K. L., Quinn, T. M., & Taylor, F. W. (2007). Reconstructing twentieth-century  
654 sea surface temperature variability in the southwest pacific: A replication study using  
655 multiple coral sr/ca records from new caledonia. *Paleoceanography*, 22(4). doi: 10  
656 .1029/2007PA001444
- 657 DeLong, K. L., Quinn, T. M., Taylor, F. W., Shen, C.-C., & Lin, K. (2013). Improving coral-  
658 base paleoclimate reconstructions by replicating 350 years of coral Sr/Ca variations.  
659 *Palaeogeography, Palaeoclimatology, Palaeoecology*, 373, 6 - 24. doi: [https://doi.org/  
660 10.1016/j.palaeo.2012.08.019](https://doi.org/10.1016/j.palaeo.2012.08.019)
- 661 D'Olivo, J. P., Georgiou, L., Falter, J., DeCarlo, T. M., Irigoien, X., Voolstra, C. R., ...  
662 McCulloch, M. T. (2019). Long-term impacts of the 1997–1998 bleaching event on the  
663 growth and resilience of massive porites corals from the central red sea. *Geochemistry,*  
664 *Geophysics, Geosystems*, 20(6), 2936-2954. doi: 10.1029/2019GC008312
- 665 D'Olivo, J. P., & McCulloch, M. (2017). Response of coral calcification and calcifying fluid  
666 composition to thermally induced bleaching stress. *Scientific Reports*, 7(1), 1–15.
- 667 Donner, S. D. (2011). An evaluation of the effect of recent temperature variability on the  
668 prediction of coral bleaching events. *Ecological Applications*, 21(5), 1718-1730. doi:  
669 10.1890/10-0107.1

- 670 Donner, S. D., Rickbeil, G. J., & Heron, S. F. (2017). A new, high-resolution global mass  
671 coral bleaching database. *PLoS One*, *12*(4), e0175490.
- 672 Fröhlicher, T. L., Fischer, E. M., & Gruber, N. (2018). Marine heatwaves under global  
673 warming. *Nature*, *560*(7718), 360–364.
- 674 Gaetani, G. A., & Cohen, A. L. (2006). Element partitioning during precipitation of  
675 aragonite from seawater: a framework for understanding paleoproxies. *Geochimica et*  
676 *Cosmochimica Acta*, *70*(18), 4617–4634.
- 677 Gagan, M. K., Dunbar, G. B., & Suzuki, A. (2012). The effect of skeletal mass accumulation  
678 in porites on coral sr/ca and  $\delta^{18}\text{O}$  paleothermometry. *Paleoceanography*, *27*(1). doi:  
679 10.1029/2011PA002215
- 680 Gibbin, E. M., Krueger, T., Putnam, H. M., Barott, K. L., Bodin, J., Gates, R. D., &  
681 Meibom, A. (2018). Short-term thermal acclimation modifies the metabolic condition  
682 of the coral holobiont. *Frontiers in Marine Science*, *5*, 10.
- 683 Glynn, P. W. (1988). El nino—southern oscillation 1982-1983: Nearshore population,  
684 community, and ecosystem responses. *Annual Review of Ecology and Systematics*,  
685 *19*(1), 309–346.
- 686 Glynn, P. W. (2000). Effects of the 1997–98 el niño southern oscillation on eastern pacific  
687 corals and coral reefs: An overview. In *Proc. 9th int. coral reef symp* (Vol. 2, pp.  
688 1169–1174).
- 689 Glynn, P. W., Feingold, J. S., Baker, A., Banks, S., Baums, I. B., Cole, J., . . . others (2018).  
690 State of corals and coral reefs of the galápagos islands (ecuador): Past, present and  
691 future. *Marine pollution bulletin*, *133*, 717–733.
- 692 Glynn, P. W., Riegl, B., Purkis, S., Kerr, J. M., & Smith, T. B. (2015). Coral reef recovery  
693 in the galápagos islands: the northernmost islands (darwin and wenman). *Coral Reefs*,  
694 *34*(2), 421–436.
- 695 Goodkin, N. F., Hughen, K. A., Cohen, A. L., & Smith, S. R. (2005). Record of little  
696 ice age sea surface temperatures at bermuda using a growth-dependent calibration of  
697 coral sr/ca. *Paleoceanography*, *20*(4). doi: 10.1029/2005PA001140
- 698 Grove, C. A., Kasper, S., Zinke, J., Pfeiffer, M., Garbe-Schönberg, D., & Brummer, G.-  
699 J. A. (2013). Confounding effects of coral growth and high SST variability on skeletal  
700 Sr/Ca: Implications for coral paleothermometry. *Geochemistry, Geophysics, Geosys-*  
701 *tems*, *14*(4), 1277-1293. doi: 10.1002/ggge.20095
- 702 Hetzinger, S., Pfeiffer, M., Dullo, W.-C., Zinke, J., & Garbe-Schönberg, D. (2016). A change  
703 in coral extension rates and stable isotopes after El Niño-induced coral bleaching and  
704 regional stress events. *Scientific Reports*, *6*, 32879.
- 705 Hoadley, K. D., Lewis, A. M., Wham, D. C., Pettay, D. T., Grasso, C., Smith, R., . . .  
706 Warner, M. E. (2019). Host–symbiont combinations dictate the photo-physiological  
707 response of reef-building corals to thermal stress. *Scientific Reports*, *9*(1), 1–15.
- 708 Hobday, A. J., Alexander, L. V., Perkins, S. E., Smale, D. A., Straub, S. C., Oliver, E. C.,  
709 . . . others (2016). A hierarchical approach to defining marine heatwaves. *Progress in*  
710 *Oceanography*, *141*, 227–238.
- 711 Hoegh-Guldberg, O. (1999). Climate change, coral bleaching and the future of the world’s  
712 coral reefs. *Marine and freshwater research*, *50*(8), 839–866.
- 713 Huang, B., Thorne, P. W., Banzon, V. F., Boyer, T., Chepurin, G., Lawrimore, J. H., . . .  
714 Zhang, H.-M. (2017, 09). Extended Reconstructed Sea Surface Temperature, Version  
715 5 (ERSSTv5): Upgrades, Validations, and Intercomparisons. *Journal of Climate*,  
716 *30*(20), 8179-8205. doi: 10.1175/JCLI-D-16-0836.1
- 717 Jimenez, G., Cole, J. E., Thompson, D. M., & Tudhope, A. W. (2018). Northern galápagos  
718 corals reveal twentieth century warming in the eastern tropical pacific. *Geophysical*  
719 *Research Letters*, *45*(4), 1981-1988. doi: 10.1002/2017GL075323
- 720 Jones, A., & Berkelmans, R. (2010). Potential costs of acclimatization to a warmer climate:  
721 growth of a reef coral with heat tolerant vs. sensitive symbiont types. *PloS one*, *5*(5),  
722 e10437.
- 723 Kessler, W. S. (2006). The circulation of the eastern tropical pacific: A review. *Progress in*  
724 *Oceanography*, *69*(2-4), 181–217.

- 725 Lawman, A. E., Partin, J. W., Dee, S. G., Casadio, C. A., Di Nezio, P., & Quinn, T. M.  
726 (2020). Developing a coral proxy system model to compare coral and climate model  
727 estimates of changes in paleo-enso variability. *Paleoceanography and Paleoclimatology*,  
728 *35*(7), e2019PA003836. doi: 10.1029/2019PA003836
- 729 Leupold, M., Pfeiffer, M., Garbe-Schönberg, D., & Sheppard, C. (2019). Reef-Scale-  
730 Dependent Response of Massive Porites Corals From the Central Indian Ocean to  
731 Prolonged Thermal Stress: Evidence From Coral Sr/Ca Measurements. *Geochem-*  
732 *istry, Geophysics, Geosystems*, *20*(3), 1468-1484. doi: 10.1029/2018GC007796
- 733 Linsley, B. K., Wu, H. C., Dassié, E. P., & Schrag, D. P. (2015). Decadal changes in south  
734 pacific sea surface temperatures and the relationship to the pacific decadal oscillation  
735 and upper ocean heat content. *Geophysical Research Letters*, *42*(7), 2358-2366. doi:  
736 10.1002/2015GL063045
- 737 Liu, G., Strong, A. E., & Skirving, W. (2003). Remote sensing of sea surface temperatures  
738 during 2002 barrier reef coral bleaching. *Eos, Transactions American Geophysical*  
739 *Union*, *84*(15), 137–141.
- 740 Logan, C. A., Dunne, J., Eakin, C., & Donner, S. (2012). A framework for comparing coral  
741 bleaching thresholds. In *Proceedings of the 12th international coral reef symposium*  
742 *(ed yellowlees d, hughes tp)*, pp 10a3 townsville [internet].
- 743 Loope, G., Thompson, D., Cole, J., & Overpeck, J. (2020). Is there a low-frequency bias  
744 in multiproxy reconstructions of tropical pacific sst variability? *Quaternary Science*  
745 *Reviews*, *246*, 106530.
- 746 Lough, J. M., & Cantin, N. E. (2014). Perspectives on massive coral growth rates in a chang-  
747 ing ocean. *The Biological Bulletin*, *226*(3), 187-202. doi: 10.1086/BBLv226n3p187
- 748 Manzello, D. P., Kleypas, J. A., Budd, D. A., Eakin, C. M., Glynn, P. W., & Langdon, C.  
749 (2008). Poorly cemented coral reefs of the eastern tropical pacific: Possible insights  
750 into reef development in a high-co2 world. *Proceedings of the National Academy of*  
751 *Sciences*, *105*(30), 10450–10455.
- 752 Marchitto, T., Bryan, S., Doss, W., McCulloch, M., & Montagna, P. (2018). A sim-  
753 ple biomineralization model to explain Li, Mg, and Sr incorporation into aragonitic  
754 foraminifera and corals. *Earth and Planetary Science Letters*, *481*, 20 - 29. doi:  
755 <https://doi.org/10.1016/j.epsl.2017.10.022>
- 756 Marshall, J. F., & McCulloch, M. T. (2002). An assessment of the Sr/Ca ratio in shal-  
757 low water hermatypic corals as a proxy for sea surface temperature. *Geochimica et*  
758 *Cosmochimica Acta*, *66*(18), 3263–3280.
- 759 McCulloch, M., D’Olivo, J. P., Falter, J., Holcomb, M., & Trotter, J. A. (2017). Coral calci-  
760 fication in a changing world and the interactive dynamics of pH and DIC upregulation.  
761 *Nature Communications*, *8*(1), 1–8.
- 762 Nothdurft, L. D., & Webb, G. E. (2007). Microstructure of common reef-building coral  
763 genera acropora, pocillopora, goniastrea and porites: constraints on spatial resolution  
764 in geochemical sampling. *Facies*, *53*(1), 1–26.
- 765 Nurhati, I. S., Cobb, K. M., Charles, C. D., & Dunbar, R. B. (2009). Late 20th century  
766 warming and freshening in the central tropical pacific. *Geophysical Research Letters*,  
767 *36*(21). doi: 10.1029/2009GL040270
- 768 Oliver, E. C., Donat, M. G., Burrows, M. T., Moore, P. J., Smale, D. A., Alexander, L. V.,  
769 ... others (2018). Longer and more frequent marine heatwaves over the past century.  
770 *Nature communications*, *9*(1), 1–12.
- 771 Palumbi, S. R., Barshis, D. J., Traylor-Knowles, N., & Bay, R. A. (2014). Mechanisms of  
772 reef coral resistance to future climate change. *Science*, *344*(6186), 895–898.
- 773 Reed, E. V., Thompson, D. M., Cole, J. E., Lough, J. M., Cantin, N. E., Cheung, A. H.,  
774 ... Edwards, R. L. (2021). Impacts of coral growth on geochemistry: Lessons from  
775 the galápagos islands. *Paleoceanography and Paleoclimatology*, *36*(4), e2020PA004051.  
776 doi: <https://doi.org/10.1029/2020PA004051>
- 777 Reynolds, R. W., Smith, T. M., Liu, C., Chelton, D. B., Casey, K. S., & Schlax, M. G. (2007,  
778 11). Daily High-Resolution-Blended Analyses for Sea Surface Temperature. *Journal*  
779 *of Climate*, *20*(22), 5473-5496. doi: 10.1175/2007JCLI1824.1

- 780 Riegl, B., Johnston, M., Glynn, P. W., Keith, I., Rivera, F., Vera-Zambrano, M., . . . Glynn,  
781 P. J. (2019a). Some environmental and biological determinants of coral richness,  
782 resilience and reef building in galápagos (ecuador). *Scientific Reports*, *9*(1), 1–16.
- 783 Sagar, N., Hetzinger, S., Pfeiffer, M., Masood Ahmad, S., Dullo, W.-C., & Garbe-Schönberg,  
784 D. (2016). High-resolution sr/ca ratios in a porites lutea coral from lakshadweep  
785 archipelago, southeast arabian sea: An example from a region experiencing steady  
786 rise in the reef temperature. *Journal of Geophysical Research: Oceans*, *121*(1), 252–  
787 266. doi: 10.1002/2015JC010821
- 788 Sayani, H. R., Cobb, K. M., DeLong, K., Hitt, N. T., & Druffel, E. R. M. (2019). Inter-  
789 colony  $\delta^{18}\text{O}$  and Sr/Ca variability among Porites spp. corals at Palmyra Atoll: Toward  
790 more robust coral-based estimates of climate. *Geochemistry, Geophysics, Geosystems*,  
791 *20*(11), 5270–5284. doi: 10.1029/2019GC008420
- 792 Schrag, D. P. (1999). Rapid analysis of high-precision sr/ca ratios in corals and other marine  
793 carbonates. *Paleoceanography*, *14*(2), 97–102. doi: 10.1029/1998PA900025
- 794 Sevilgen, D. S., Venn, A. A., Hu, M. Y., Tambutté, E., de Beer, D., Planas-Bielsa, V., &  
795 Tambutté, S. (2019). Full in vivo characterization of carbonate chemistry at the site  
796 of calcification in corals. *Science advances*, *5*(1), eaau7447.
- 797 Sinclair, D. J. (2015). Rbme coral temperature reconstruction: An evaluation, modifications,  
798 and recommendations. *Geochimica et Cosmochimica Acta*, *154*, 66–80.
- 799 Sully, S., Burkepille, D., Donovan, M., Hodgson, G., & Van Woesik, R. (2019). A global  
800 analysis of coral bleaching over the past two decades. *Nature communications*, *10*(1),  
801 1–5.
- 802 Thirumalai, K., Singh, A., & Ramesh, R. (2011). A matlab<sup>TM</sup> code to perform weighted  
803 linear regression with (correlated or uncorrelated) errors in bivariate data. *Journal of*  
804 *the Geological Society of India*, *77*(4), 377–380.
- 805 Thompson, D. M. (n.d.). Environmental records from coral skeletons: a decade of novel  
806 insights and innovation. *WIREs Climate Change*. doi: 10.1002/wcc.745
- 807 Thompson, D. M., & van Woesik, R. (2009). Corals escape bleaching in regions that recently  
808 and historically experienced frequent thermal stress. *Proceedings of the Royal Society*  
809 *B: Biological Sciences*, *276*(1669), 2893–2901. doi: 10.1098/rspb.2009.0591
- 810 Tierney, J. E., Abram, N. J., Anchukaitis, K. J., Evans, M. N., Giry, C., Kilbourne, K. H.,  
811 . . . Zinke, J. (2015). Tropical sea surface temperatures for the past four centuries  
812 reconstructed from coral archives. *Paleoceanography*, *30*(3), 226–252. doi: 10.1002/  
813 2014PA002717
- 814 Wellington, G. M., & Glynn, P. W. (1983). Environmental influences on skeletal banding  
815 in eastern pacific (panama) corals. *Coral reefs*, *1*(4), 215–222.
- 816 Wu, H. C., Moreau, M., Linsley, B. K., Schrag, D. P., & Corrège, T. (2014). Investigation of  
817 sea surface temperature changes from replicated coral Sr/Ca variations in the eastern  
818 equatorial Pacific (Clipperton Atoll) since 1874. *Palaeogeography, Palaeoclimatology,*  
819 *Palaeoecology*, *412*, 208–222.
- 820 York, D., Evensen, N. M., Martinez, M. L., & De Basabe Delgado, J. (2004). Unified equa-  
821 tions for the slope, intercept, and standard errors of the best straight line. *American*  
822 *Journal of Physics*, *72*(3), 367–375.
- 823 Ziegler, M., Seneca, F. O., Yum, L. K., Palumbi, S. R., & Voolstra, C. R. (2017). Bac-  
824 terial community dynamics are linked to patterns of coral heat tolerance. *Nature*  
825 *communications*, *8*(1), 1–8.